

Article

Research on Passive Design Strategies for Low-Carbon Substations in Different Climate Zones

Shuizhong Zhao ¹, Jiangfeng Si ¹, Gang Chen ¹, Hong Shi ¹, Yusong Lei ², Zhaoyang Xu ³ and Liu Yang ^{4,*}

¹ State Grid Huzhou Electric Power Supply Company State Grid Zhejiang Electric Power Supply Company, LTD, Huzhou 313000, China; zhaoshuizhong@sgepri.sgcc.com.cn (S.Z.); sjiangfeng@sgepri.sgcc.com.cn (J.S.); chengang@sgepri.sgcc.com.cn (G.C.); shihong@sgepri.sgcc.com.cn (H.S.)

² Huzhou Electric Power Design Institute Co., Huzhou 313000, China; leiyusong@sgepri.sgcc.com.cn

³ State Grid Electric Power Research Institute Wuhan Efficiency Evaluation Co., Ltd., Wuhan 430077, China; xuzhaoyang@sgepri.sgcc.com.cn

⁴ College of Civil Engineering and Architecture, Henan University of Technology, Zhengzhou 450001, China

* Correspondence: yl@haut.edu.cn; Tel.: +86-186-2371-2023

Abstract: In the energy-saving design of substations, the building envelope thermal parameters, window-to-wall ratio, and shape factor are three crucial influencing factors. They not only affect the building's appearance but also have an important impact on the total building energy consumption. In this paper, we applied the energy consumption simulation software DeST-c to study the influence of the above three elements on the total energy consumption of the building in a representative city with different thermal zones. The optimal envelope thermal parameters, optimal window-to-wall ratio, and optimal shape factor were derived through combination with economic analysis. Finally, the sensitivity analysis of different elements was carried out to determine the suitable passive design solutions for substations in different climate zones. It was found that the thickness of roof insulation has the greatest influence on the energy consumption of substation buildings among all envelopes. The optimal window-to-wall ratios were 0.4, 0.4~0.5, 0.3, 0.3~0.4, and 0.5 for severe cold, cold, hot summer and cold winter, hot summer and warm winter, and mild regions, respectively; and the optimal shape factors were 0.29, 0.30, 0.23, 0.31, and 0.33, respectively. The conclusions of this study can provide architects with energy-saving design strategies and suggestions for substations in different climate zones, and provide references for building energy-saving designs and air conditioning and heating equipment selection.

Keywords: low-carbon substation; climate zones; envelope thermal design; window to wall ratio; shape factor



Citation: Zhao, S.; Si, J.; Chen, G.; Shi, H.; Lei, Y.; Xu, Z.; Yang, L. Research on Passive Design Strategies for Low-Carbon Substations in Different Climate Zones. *Processes* **2023**, *11*, 1814. <https://doi.org/10.3390/pr11061814>

Academic Editors: Yabin Guo, Zhanwei Wang, Yunpeng Hu and João M. M. Gomes

Received: 23 April 2023

Revised: 9 June 2023

Accepted: 10 June 2023

Published: 14 June 2023



Copyright: © 2023 by the authors. Licensee MDPI, Basel, Switzerland. This article is an open access article distributed under the terms and conditions of the Creative Commons Attribution (CC BY) license (<https://creativecommons.org/licenses/by/4.0/>).

1. Introduction

Currently, global energy demand is rising dramatically, and electricity consumption has increased 3.9 times since 1973 [1,2]. In order to mitigate global warming and achieve carbon peak and carbon neutrality, significant decarbonization of the global energy system has become the key to the sustainability of the world [3]. As the main part and key node of the power grid, substations have high energy consumption and a lack of energy-saving concepts in their design, resulting in serious energy wastage [4,5]. Therefore, the energy-saving design of substations is a crucial step to reduce carbon emissions [6].

With the growth of electricity consumption in recent years, the number of substations has gradually increased, and they are widely distributed with various building facilities [7]. According to the category of buildings, substation buildings belong to industrial buildings [8,9], and their construction process must meet the requirements of both electrical processes and special buildings, and also requires comprehensive consideration of various technical requirements, such as lighting, ventilation, and fire protection [10]. Therefore, compared with ordinary industrial buildings, substation buildings are characterized by

higher energy consumption, high environmental control requirements, and complex energy consumption influencing factors [11]. Meanwhile, detailed energy-saving regulations have not been made for industrial buildings, especially substation buildings [12]. In addition, their design process takes less consideration of comfort issues such as indoor dehumidification [13] and energy consumption of air conditioning systems [14] and lacks the concept of energy saving. Therefore, it is desirable to carry out passive energy-saving designs for them.

Passive buildings are developed on the basis of low-energy buildings. The so-called passive building refers to the use of materials with higher insulation performance and windows and doors with lower heat transfer coefficients, the use of optimized building construction practices to achieve efficient thermal insulation performance, and the use of clean energy to provide heating or cooling to the room, reducing or eliminating the use of actively supplied energy to make the building reach the requirements of a comfortable temperature. Passive buildings can save more than 80–90% of energy compared to conventional buildings. Passive building technology has become the most effective way to reduce building energy consumption, lower carbon emissions, and improve indoor thermal comfort [15–17]. Therefore, it has received wide attention from scholars in recent years. The main technical routes for realizing passive buildings include thermal bridge-free design and construction, rational arrangement of building orientation, design of building openings that facilitate natural ventilation, thermal insulation technology for the building envelope, building shading technology, energy-efficient windows and doors [18], building body shape, optimal window-to-wall ratios, and renewable energy use. Among them, the optimization of the envelope's thermal performance is one of the most effective methods for building energy saving. Kini et al. [19] used passive design solutions in the building envelope in warm and humid regions of India. The study showed that the envelope design improved the indoor thermal environment by 5.82 °C on a typical summer day and saved 77% of cooling energy throughout the year. Mushtaha et al. [20] conducted a passive design based on simulation methods for temperate climate zones in Palestine, including measures such as natural ventilation, external shading, and building envelope insulation. The results showed that passive design reduced building energy consumption by 59%. Jung et al. [21] studied passive design strategies for multi-story buildings in Korea. In the process, the energy, environmental impact, and economic feasibility of the dwelling could be improved by 52.7%, 39.5%, and 36.9%, respectively. Optimization of the window-to-wall ratio and shape factor of buildings are also common approaches for passive building technologies. Pajek et al. [22] investigated the effect of different passive design measures such as thermal transmittance, window-to-wall ratio, and window distribution on energy use in single-family residential buildings for a representative European climate. It was found that zero-energy buildings may be obtained in Porto by appropriate passive design. Li et al. [23] aimed to improve the indoor environment by utilizing solar energy in existing residential buildings in Lhasa, increasing the window-to-wall ratio on the south wall while reducing the depth of south-facing rooms and increasing the width of bays. Yin [24] evaluated the energy performance of passive buildings in typical cities in three climate zones in China and concluded that a smaller shape factor could lead to lower energy consumption. Zhang [25] found that energy consumption increased by 5%, 10%, and 20% when the building shape factor increased from 0.30 to 0.32, 0.34, and 0.36, respectively, through a study of existing buildings.

Passive building technology is also relatively widely used in substations. Kang et al. [26] discussed energy-saving measures for substations in severe cold regions in terms of building exterior walls, roofs, doors, and windows, respectively. It was concluded that energy-saving designs can reduce the total energy consumption of heating, ventilation, air conditioning, and lighting by 50% throughout the year. Zhang et al. [27] used a passive design concept for an extra-high voltage substation in Shijiazhuang, which led to an 85% energy saving in the building through the design of the exterior insulation system and airtightness design. Nie et al. [12] discovered that, based on the climatic conditions in Inner Mongolia,

the energy-saving designs of the building's general plan, walls, windows, and roofs can achieve better building energy saving. Yang [28] studied the ventilation and air conditioning system of the Expo substation and obtained an optimized energy-saving solution by changing parameters such as air supply method, height, and effective area of air outlets. Wang et al. [29] proposed a joint centralized operation of air conditioners and exhaust fans based on the self-control strategy of the substation air conditioning system, which eventually reduced the electricity consumption of the substation. Xiong et al. [30] used passive design to enhance natural ventilation and reduce building energy demand based on field research and DeST software simulation. Zhang [31] achieved excellent economic, social, and environmental benefits by controlling the substation building shape factor and designing energy-saving strategies for exterior walls, roofs, windows, and doors. Liu et al. [32] conducted a dynamic energy consumption simulation of the Guangzhou substation by DeST-C to analyze the influence of thermal parameters of the exterior envelope on air conditioning energy consumption in the absence of natural ventilation. It was found that the building's air conditioning energy consumption decreased with increasing heat transfer coefficients of exterior walls, roofs, and exterior windows. Zhou [33] analyzed the building energy-saving design points of the Kunming substation from general layout optimization, reasonable building layout and functional zoning optimization, the energy-saving design of the envelope, and ventilation design. Zhang et al. [34] took the substation building in the Wenzhou area as the research object, analyzed the building energy consumption of the substation, and proposed specific measures for energy saving in terms of substation building monolith, shape factor, and envelope, which effectively reduced the substation's building energy consumption. Zhang et al. [35] calculated the heat dissipation of electrical equipment by collecting the internal and external temperatures of the substation building and testing the heat transfer coefficient of the enclosure system. It provided a basis for the overall design scheme of energy saving in substation buildings in severely cold regions.

Through the existing literature, it can be found that although there were some studies on substations, most of them only proposed some energy-saving methods without giving specific optimized design parameters and did not take into consideration the window-to-wall ratio and shape factors. At the same time, there were few references for the research on the energy-saving indexes of substation buildings, and there were only a few thermal performance tests of substation buildings and guidance for energy-saving design work of substation buildings. Therefore, in this study, typical cities in five climate zones, namely (a) severe cold, (b) cold, (c) hot summer and cold winter, (d) hot summer and warm winter, and (e) mild, were selected, and the optimal envelope thermal parameters, optimal window-to-wall ratio, and optimal shape factors for each climate zone were derived by controlling variables and using DeST-c simulation. The regression equations and errors of total building energy consumption versus window-to-wall ratio and total energy consumption versus shape factors were also obtained. Finally, combined with sensitivity analysis, the optimal design strategies for each climate zone were obtained. The study provides a reference basis for the design scheme of substation buildings and provides data support for the construction of 220 kV substations in different climate zones.

This paper is structured as follows: Section 2 first analyzed the key impact parameters of the substation building and determined the economic evaluation index. Then simulation tools, climate zones, and thermal disturbance parameters were selected to build a physical model of the substation; Section 3's energy simulation yielded results for a simple analysis; Section 4 derived the optimal design solutions for the thermal characteristics of the envelope, the window-to-wall ratio, and shape factor in each region; Section 5 concluded the study.

2. Methodology

In this study, using the energy consumption simulation software DeST-c applied to commercial buildings, the technical route of the study was shown in Figure 1. First, on-site research was conducted on several substations to establish a typical substation building model by using thermal disturbance parameters, thermal parameters, and building

information. Then, using the control variable method, the total energy consumption of the substation building was derived by varying the envelope heat transfer coefficient, window-to-wall ratio, and shape factor, respectively, in the simulation. Then, the optimal window-to-wall ratio and optimal shape factor were obtained based on the energy consumption level, and the optimal envelope thermal parameters also needed to be combined with the Benefits-to-Cost Ratio (R_{BC}). Finally, a sensitivity analysis was performed to determine the optimal optimization strategy for substations in different climate zones.

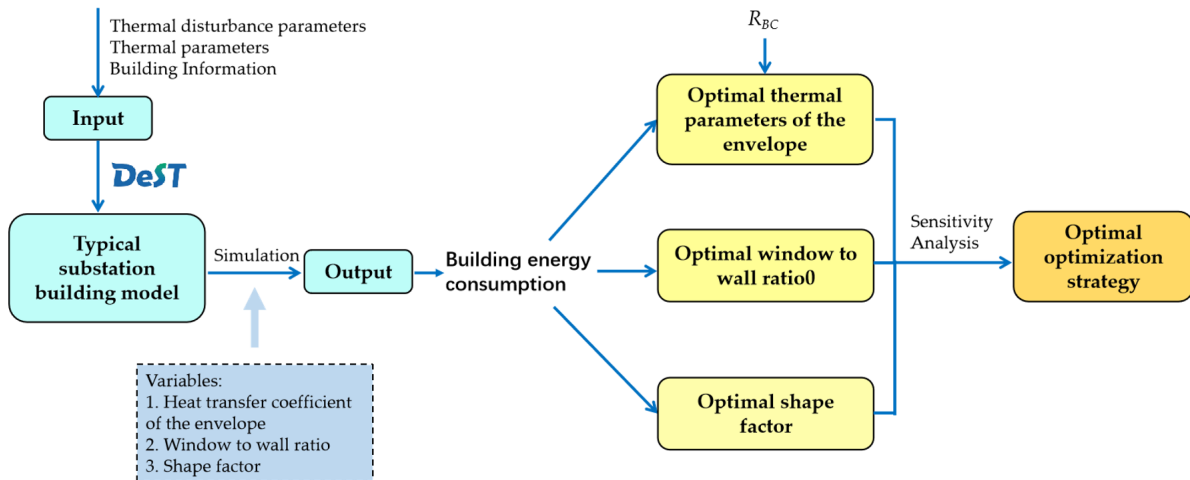


Figure 1. Technology Roadmap.

2.1. Analysis of Key Impact Parameters of Passive Energy Saving in Substation Buildings

First, a theoretical analysis of the heat transfer process of the substation building was carried out to obtain the key influencing factors of energy consumption in the substation building. As shown in Figure 2, in addition to the energy consumption of the production equipment itself, the main energy consumption of the substation building was the energy consumption of the air conditioning system needed to maintain the normal operation of the production equipment and the thermal comfort of the personnel on duty.

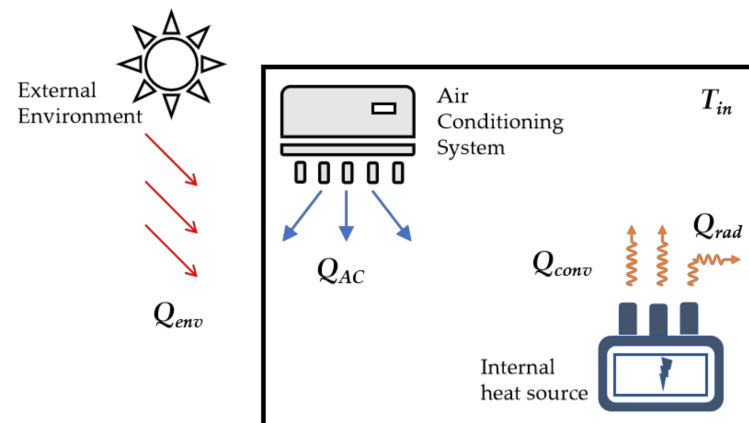


Figure 2. Schematic diagram of heat transfer in substation building. Note: T_{in} is the indoor air temperature, K; Q_{env} is the heat transfer from the envelope to the room, kW; Q_{conv} is the convection heat dissipation from the indoor heat source, kW; Q_{rad} is the radiation heat dissipation from the indoor heat source, kW; Q_{AC} is the heat supplied to the room by the air conditioning system, kW.

According to the heat transfer from the envelope of the substation and the internal heat source, the indoor heat balance equation of the substation was listed as Equation (1). Among them, the heat dissipation from indoor heat sources was divided into two parts, convection and radiation. However, only the convection part could directly heat the indoor

air, while the radiation part was heating other solid surfaces first, and then transmitting to the air by convection. Therefore, only the convection part of the indoor heat source could be reflected in Equation (1).

$$\rho_{in} V_{in} c_{in} \frac{\partial T_{in}}{\partial t} = \sum Q_{env} + \sum Q_{conv} + \sum Q_{AC} \tag{1}$$

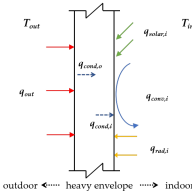
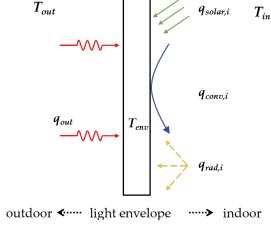
where, ρ_{in} is the indoor air density, kg/m³; V_{in} is the indoor air volume, m³; c_{in} is the specific heat of air, kJ/kg·K; t is the time analyzed, s.

As can be seen, for substation buildings, their production equipment and staff were necessary for their normal working configuration, so the heat dissipation $\sum Q_{conv}$ from indoor heat sources cannot be regulated. Therefore, if we want to reduce the energy consumption of the substation, i.e., reduce the extra heat added or removed $\sum Q_{AC}$, we must try to control the heat transfer $\sum Q_{env}$ of the building envelope.

The heat transfer of the building envelope was further analyzed to establish a set of dynamic heat transfer equations.

Outer envelopes such as exterior walls and roofs were usually analyzed according to one-dimensional unsteady heat transfer. For a less heat-indolent envelope such as windows, the heat storage effect was usually ignored in the heat transfer analysis, and they were analyzed according to the steady-state heat transfer process. The heat transfer diagram and heat balance equation are shown in Table 1.

Table 1. Heat transfer in the substation’s building envelope.

Envelope	Heavy Envelope	Light Envelope
Heat transfer diagram		
Heat balance relationship	outer surface: $q_{out} = q_{cond,o}$ (2) inner surface: $q_{cond,i} + q_{solar,i} + q_{rad,i} = q_{conv,i}$ (3) Unsteady thermal conduction: $\frac{\partial T_{env}}{\partial t} = a_{env} \frac{\partial^2 T_{env}}{\partial x_{env}^2}, 0 \leq x_{env} \leq \sigma_{env}, t > 0$ (4)	$q_{out} + q_{solar,i} + q_{rad,i} = q_{conv,i}$ (6)
Expanding equations	$-\lambda_{env,o} \left(\frac{\partial T_{env}}{\partial x_{env}} \right)_{x_{env}=0} = \alpha_{env} (T_{out} - T_{env,o})$ $-\lambda_{env,i} \left(\frac{\partial T_{env}}{\partial x_{env}} \right)_{x_{env}=\sigma_{env}} + \gamma_{env} Q_{solar,i} / A_{env} + \alpha_{env,rad,i} (T_{env,i} - T_{ave,i}) + \kappa_{env} Q_{rad} / A_{env} = \alpha_{env,i} (T_{env,i} - T_{in})$ (5)	$\alpha_{env,o} (T_{out} - T_{env}) + \gamma_{env} Q_{solar,i} / A_{env} + \alpha_{env,rad,i} (T_{env} - T_{ave,i}) + \kappa_{env} Q_{rad} / A_{env} = \alpha_{env,i} (T_{env} - T_{in})$ (7)
Notes	q_{out} denotes the total heat gain of the outer surface, W/m ² ; $q_{cond,o} / q_{cond,i}$ denotes the heat gains from thermal conduction of the outer/inner surface, W/m ² ; $q_{solar,i}$ indicates the heat from sunlight entering the room with windows on the inner surface, W/m ² ; $q_{rad,i}$ denotes the heat obtained from the inner surface by radiation from an internal heat source, W/m ² ; $q_{conv,i}$ denotes the convective heat exchange between the inner surface and the room air, W/m ² ; $T_{env,o} / T_{env,i}$ indicates the outer/inner surface temperature of the envelope, K; $T_{ave,i}$ denotes the average temperature of the envelope, K; a_{env} denotes the heat diffusion coefficient, m ² /s; σ_{env} denotes the thickness of this envelope, m; $\lambda_{env,o} / \lambda_{env,i}$ denotes the thermal conductivity of the outer/inner surface, W/m·K; γ_{env} denotes the proportion of solar radiation received by the inner surface to the total incident radiation; $\alpha_{env,rad,i}$ denotes the radiation heat transfer coefficient of the inner surface, W/m ² ·K; κ_{env} denotes is the ratio of the radiant heat transfer from indoor heat sources received by the inner surface to the total radiant heat dissipation from indoor heat sources. See Nomenclature for detailed explanation.	

Through the above theoretical analysis, it could be found that the heat transfer of the outer envelope, driven by the temperature difference between indoors and outdoors, was mainly determined by the area and thermal parameters of the envelope. For functional buildings such as substations, their internal use space was usually required for production equipment and functions, which could hardly be changed. Therefore, the building shape factor (the ratio between the area of the outer surface of the building in direct contact with the outdoor atmosphere and its enclosed volume) became one of the main influences on the heat transfer of the building. The windows were less heat-indolent and easily

transformed into cold and hot bridges for heat transfer. The overall window-to-wall ratio of the building envelope determined the percentage of window area under the same total area of the envelope. In summary, “envelope thermal parameters”, “window-to-wall ratio”, and “shape factor” were selected as key parameters for passive optimization in this study. The impact of the changes in the above parameters on the energy consumption of substation buildings was studied.

2.2. Definition of the Economic Evaluation Index

By changing the thickness of the insulation layer of the envelope, the thermal performance of the building will be improved and the energy consumption of the building will be reduced accordingly. However, after the energy consumption is reduced to a certain degree, if the thickness of the insulation layer continues to be changed blindly, the speed of energy consumption reduction will be slowed down significantly, and the initial investment in the building will continue to increase [36]. Therefore, in the building design period, we should not blindly increase the thickness of the insulation layer to achieve the purpose of saving energy. Instead, it should be combined with the economic index to seek the optimal design parameters to achieve the purpose of saving energy and money.

When the thickness of the insulation layer of the initial model envelope is changed, the initial investment of the building will increase, i.e., incremental costs will be generated. The reduction in energy consumption will bring corresponding incremental economic benefits.

When the thickness of the insulation layer of the initial model envelope is changed, the initial investment of the building will increase, i.e., incremental costs will be generated, and the reduction of energy consumption will bring corresponding incremental economic benefits. Incremental costs and economic benefits are related in all phases of the building life cycle, and the Benefits-to-Cost Ratio (R_{BC}) can be used as an economic evaluation index. R_{BC} is the ratio of the total present value of benefits to the total present value of costs of the project over the calculation period and can be calculated according to Equation (8) [37].

$$R_{BC} = \frac{\sum_{t=0}^N B_t(1+d)^{-t}}{\sum_{t=0}^N C_t(1+d)^{-t}} = \frac{LCB}{LCC} \quad (8)$$

$$LCC = \sum_{t=0}^N \frac{C_t}{(1+d)^t} \quad (9)$$

$$LCB = \sum_{t=0}^N \frac{B(1+e)^t}{(1+d)^t} \quad (10)$$

where, N —the calculation period, taken as $N = 50$, i.e., the life cycle of the technical solution; t —year; B —savings in energy costs, i.e., economic benefits, B_t —economic benefits in the year t ; C —cost, C_t — the cost in the year t . $t = 0$, C_0 represents the initial costs; $t = N$, C_N represents the dismantling costs; $0 < t < N$, C_t represents the operation and maintenance costs; d —social discount rate, taken as $d = 6\%$; LCB —Life Cycle Benefits; LCC —Life Cycle Costs; e — the average annual growth rate of energy prices, take $e = 0.04$.

When the R_{BC} is greater than or equal to 1, the total present value of the benefits of the project is greater than the total present value of its costs. Therefore, it is reasonable to invest in the project. On the contrary, if R_{BC} is less than 1, then the economic efficiency of investing in the project is not at an acceptable level. The larger the value of R_{BC} , the higher the economic efficiency that the project can obtain at a certain present value of cost, in other words, the project is more profitable and more worthy of investment.

2.3. Simulation Study

(1) Selection of Simulation Tools

The study of energy consumption impact factors of substations was one of the important elements of this paper's research, i.e., the analyzed impact of different optimization strategies on the change in building energy consumption. Through a large number of actual engineering tests, the building energy simulation software can quickly solve the simulation results of energy consumption brought by different variables. At the same time, it could calculate the actual situation of building energy consumption more accurately by analyzing the change in building energy consumption with each impact factor that had a high reference value. DeST is the mainstream energy consumption simulation software in China. Its official website is <https://www.dest.net.cn/> (accessed on 22 April 2023). DeST simulates the year-round time-by-time temperatures and humidity in each room of a building in a specified area, taking into account solar radiation, multi-room relationships, inter-radiation between wall surfaces, time-by-time internal disturbances, atmosphere, and earth. The meteorological data required for the simulations are generated by Medpha, which calculates day-by-day meteorological data based on 30 years of measured meteorological data using the time-series analysis method of stochastic processes according to the principles of the time-by-time meteorological model, and further uses the ARMA model and Markov transfer matrix to perform time-by-time calculations on the basis of the day-by-day data, taking into account the interactions and time-series relationships of various meteorological parameters [38]. The time series relationship of various meteorological parameters is considered, and various topographic features of the country are corrected. It can truly reflect the climatic conditions in different regions under different months and has a high degree of simulation. In addition, the software relies on the AutoCAD platform and is relatively easy to use and highly visualized. The reliability of the simulation calculation results is confirmed by the theoretical calibration of the software and the simulation calibration with the internationally recognized building energy simulation software [39]. It was the focus of this paper to analyze the energy consumption impact factors of low-carbon substations based on DeST and propose passive design strategies.

(2) Selection of simulated climate zones

China has a vast territory, and the "Thermal Design Code for Civil Buildings" [40] (GB50176-2016) divides the country into five climatic zones: severe cold, cold, hot summer and cold winter, hot summer and warm winter, and mild. Through literature combing, it was found that the meteorological parameters in different climate zones had significant differences. Therefore, the energy-saving optimization strategies of their substations were also significantly different. In this paper, representative cities located in five different climate zones were selected: Harbin (located in the severe cold region), Beijing (located in the cold region), Wuhan (located in the hot summer and cold winter region), Guangzhou (located in the hot summer and warm winter region), and Kunming (located in the mild region). The geographical location of each city and the average daily dry bulb temperature throughout the year were shown in Figure 3.

(3) Establishment of the physical model of the substation

The initial model was established through on-site research of several substations, and its floor plan and axonometric drawing are shown in Figures 4 and 5. The model was a 220 kV internal guarded and unmanned substation with a construction area of 760 m² and a floor height of 3.6 m. The main functional rooms were the equipment room, pump room, battery room, office, data room, guard room, and bathroom, etc. The building information is shown in Table 2.

In this regard, the shape factor is the ratio of the exterior area of the building in contact with the outdoor atmosphere to the volume it encloses. The exterior surface area does not include the area of the floor and the interior wall of the unheated stairwell and the door of the house. The window-to-wall ratio is the ratio of the total area of exterior windows (including transparent curtain walls) of a certain orientation to the total area

of walls (including window area) of the same orientation. The building scheme was basically similar to the completed outdoor-type substation, and it had a certain reference and representativeness for the study of energy-saving designs of substation buildings.

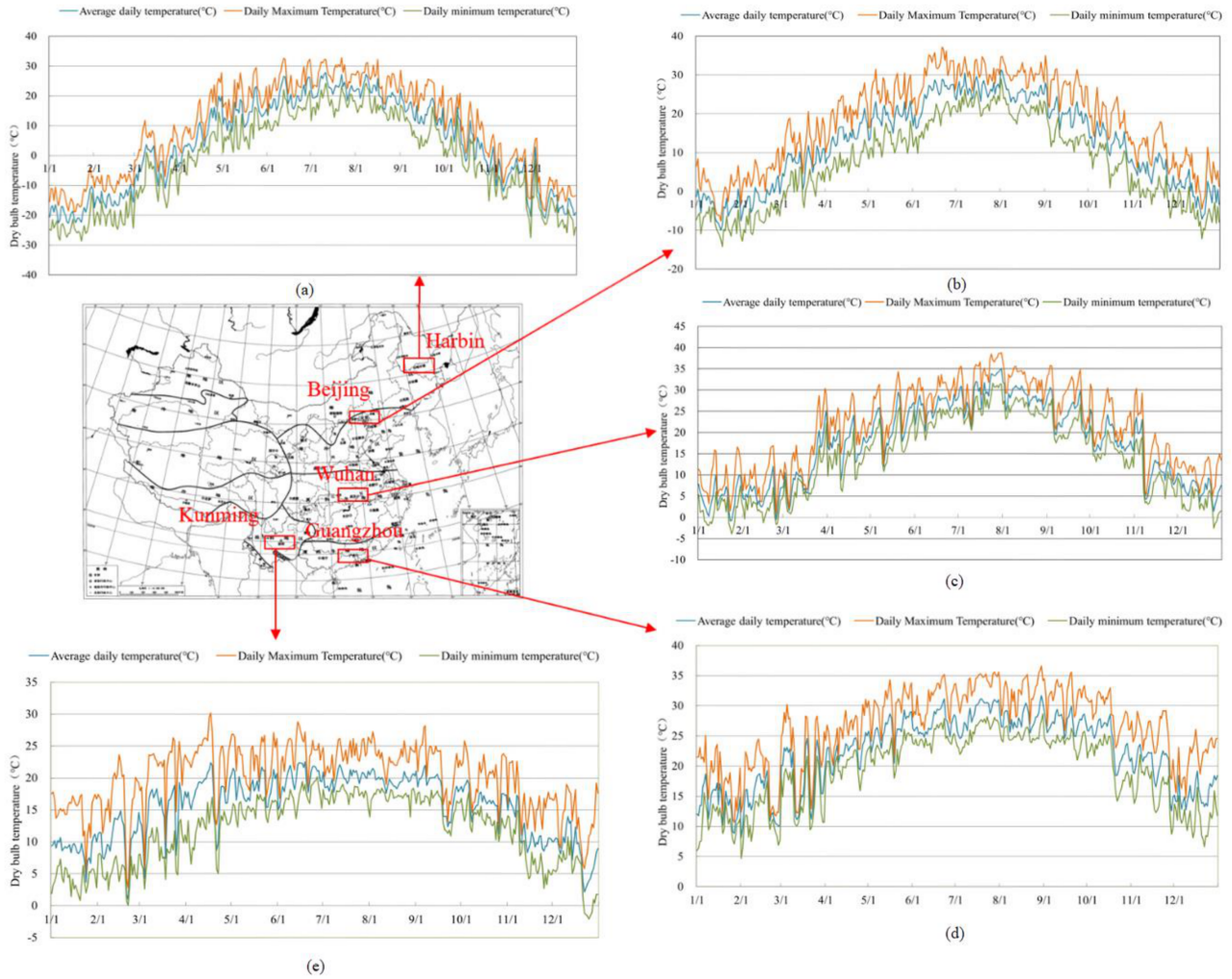


Figure 3. Geographical locations of different cities and the variation in daily average dry bulb temperatures. ((a) Harbin, (b) Beijing, (c) Wuhan, (d) Guangzhou, (e) Kunming).

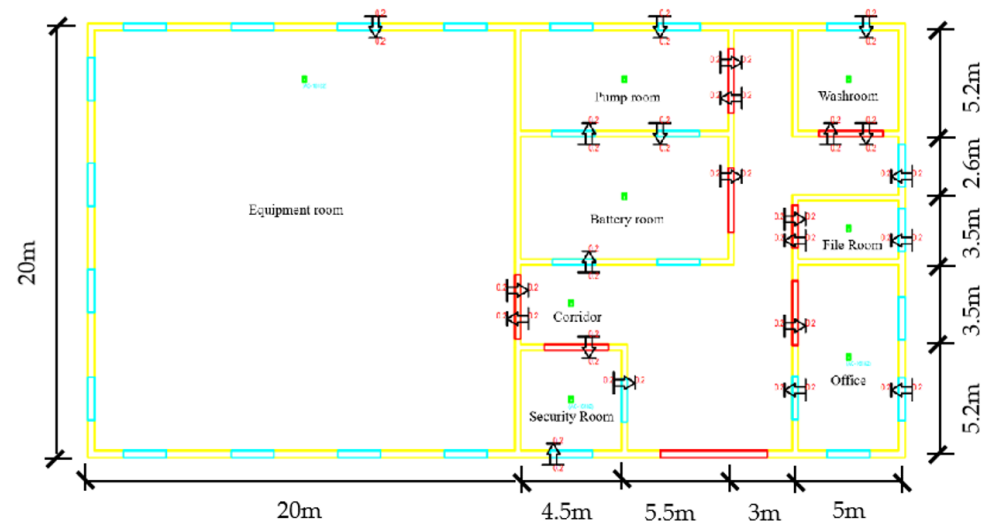


Figure 4. Substation model plan.

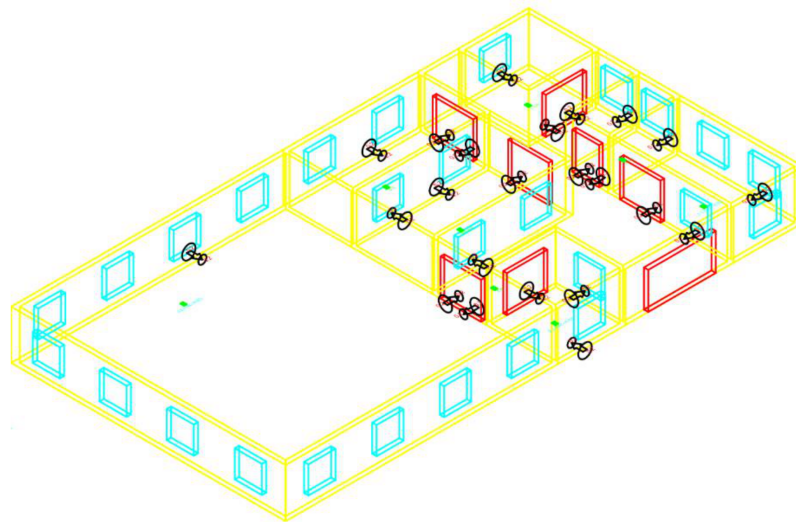


Figure 5. Axonometric drawing of the substation model.

Table 2. Initial model building information table.

Building Height/m	Building Area/m ²	Shape Factor	Window to Wall Ratio (East)	Window to Wall Ratio (South)	Window to Wall Ratio (West)	Window to Wall Ratio (North)
3.6	760	0.33	0.26	0.38	0.26	0.39

The construction of the envelope of the low-carbon substation was summarized through on-site research. Meanwhile, the material and thermal parameters of the model were set with the actual situation. As shown in Table 3.

(4) Determining the boundary conditions and working conditions of the model

The energy consumption simulation of substation buildings differed from that of other types of buildings, mainly because the internal disturbance parameters of each room were different. Through on-site research and combined with the “Technical Regulations for the Design of 220–750 kV Substation” [41] (DL/T 5218-2012), rooms in substations were classified into three categories according to the frequency of personnel activities: areas of frequent personnel activities (such as offices and guard rooms), areas of general personnel activities (such as data rooms, battery rooms, and bathrooms), and areas of electrical equipment (such as pump rooms and equipment rooms). Different types of rooms had different thermal disturbance settings. The thermal disturbance settings were as follows:

Personnel thermal disturbance: maximum number of people 1, minimum number of people 0, heat per capita 66 W, moisture production per capita 0.102, minimum fresh air per capita 30 m³/hr. Thermal disturbance allocation mode: default personnel thermal disturbance. Indicator type: square meter indicator.

Light thermal disturbance: maximum power 18 W, minimum power 0 W, electric heat conversion efficiency 0.9. Thermal disturbance allocation mode: default light thermal disturbance. Indicator type: square meter indicator.

Equipment thermal disturbance 1: maximum power 13 W, minimum power 0 W. Thermal disturbance allocation mode: default equipment thermal disturbance. Indicator type: square meter indicator. (Applicable to the areas of frequent personnel activities and general personnel activities).

Equipment thermal disturbance 2: maximum power 100 W, minimum power 0 W. Thermal disturbance allocation mode: default equipment thermal disturbance. Indicator type: square meter indicator. (Applicable to area of electrical equipment).

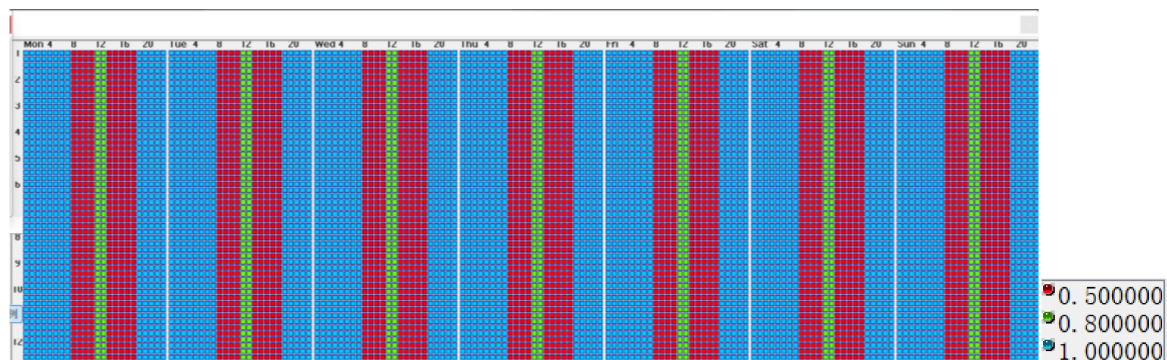
Air conditioning thermal disturbance: the upper limit of the air conditioning start temperature was 26 °C, and the lower limit of the air conditioning start temperature was

18 °C. (Only the area of frequent personnel activities and the area of electrical equipment are set up with air conditioners). The air conditioner turned on when the indoor temperature reached the air conditioner start temperature.

Table 3. Initial model thermal parameters.

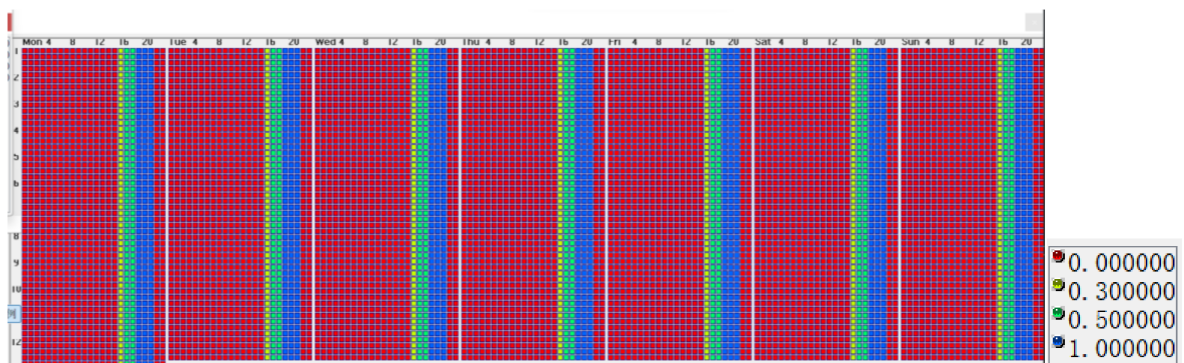
Envelope	Area (m ²)	Structure	Heat Transfer Coefficient (W/m ² ·K)
Exterior Walls	322.8	240 mm mortar clay + 10 mm pure gypsum board + 60 mm polystyrene foam + 8 mm pure gypsum board	0.564
Exterior Windows	84	3 mm flat glass + 20 mm air laminated + 3 mm flat glass	2.8
Roof	760	20 mm cement mortar + 200 mm reinforced concrete + 46 mm polystyrene + 20 mm cement mortar	0.595
Floor	760	20 mm cement mortar + 200 mm porous concrete	1.02
Exterior Door	10	25 mm pine and spruce	3.5
Interior Wall	200	20 mm cement mortar + 180 mm vitrified concrete + 20 mm cement mortar	1.515
Interior Door	40	25 mm pine and spruce	3.5
Interior Window	24	3 mm flat glass + 20 mm air laminated + 3 mm flat glass	2.8

Through inquiries and surveys of station personnel, a table of parameters for each thermal disturbance at work and rest in accordance with the substation was summarized. According to the set series of internal disturbance parameters, a complete set of frameworks for substation energy consumption simulation was formed by entering personnel thermal disturbance, light thermal disturbance, and equipment thermal disturbance, respectively, into the parameter interface. Each small square in the heat disturbance diagram represented an hourly set value, vertically by week, from the first week of January until the last week of December; horizontally by hour, from 0:00 on Monday until 23:00 on Sunday. Different colors in the figure indicated different work or usage frequencies, including the rate of fixture turn-on, equipment utilization, and occupancy of people in the room. Specific legends were marked in the figures. The larger the number, the higher the frequency of work or use. The thermal disturbance settings of the model were shown in Figures 6–9.

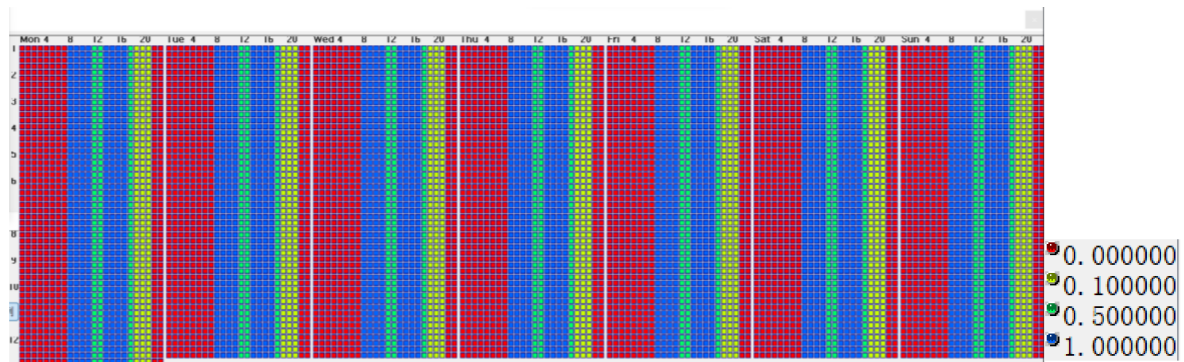


(a)

Figure 6. Cont.



(b)

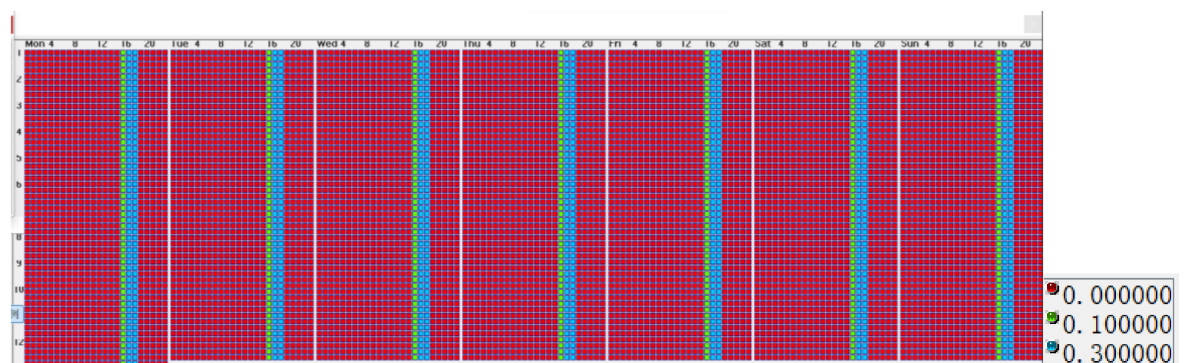


(c)

Figure 6. Thermal disturbance settings in areas of frequent personnel activities: (a) Personnel thermal disturbance, (b) Light thermal disturbance, (c) Equipment thermal disturbance.

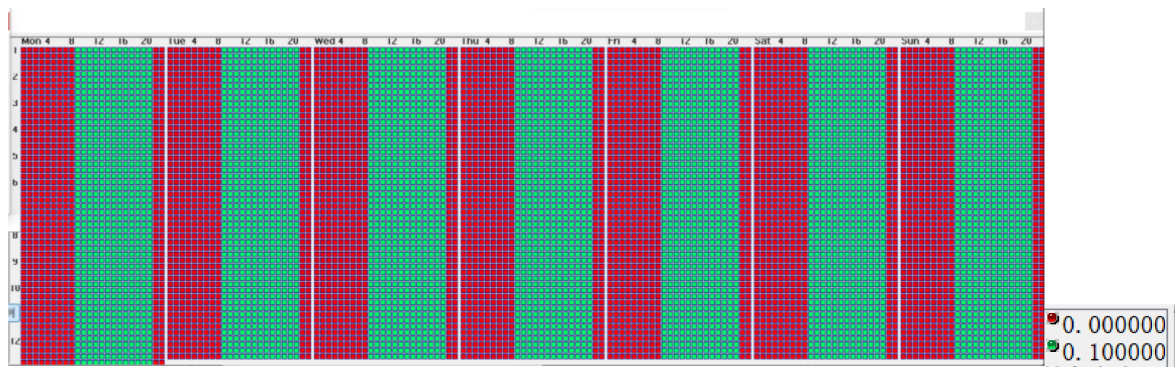


(a)



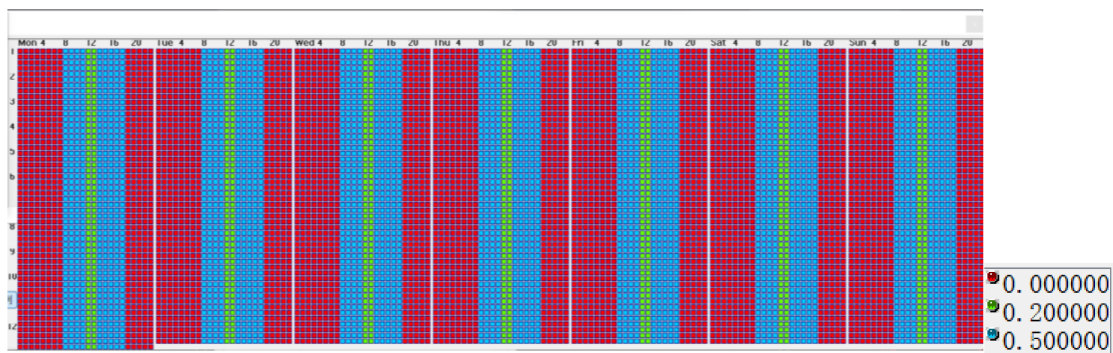
(b)

Figure 7. Cont.

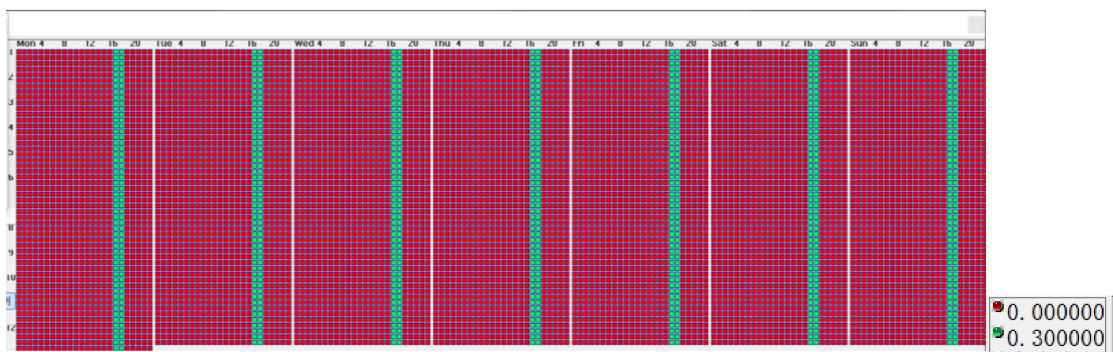


(c)

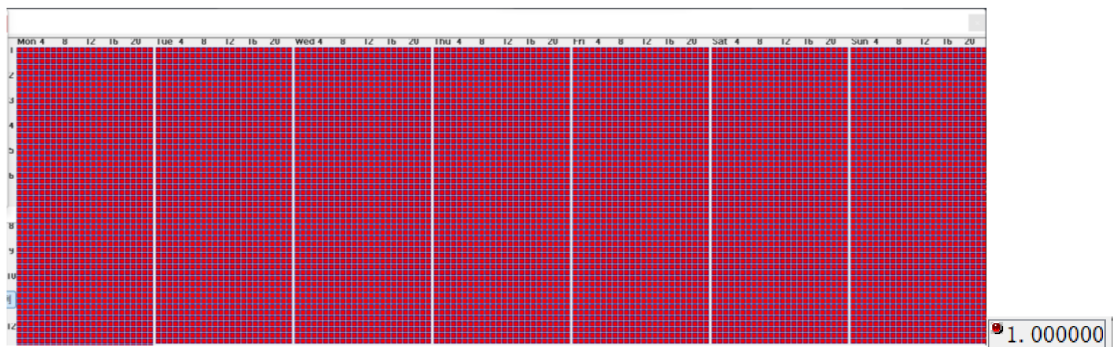
Figure 7. Thermal disturbance settings in areas of general personnel activities: (a) Personnel thermal disturbance, (b) Light thermal disturbance, (c) Equipment thermal disturbance.



(a)



(b)



(c)

Figure 8. Thermal disturbance settings in areas of electrical equipment: (a) Personnel thermal disturbance, (b) Light thermal disturbance, (c) Equipment thermal disturbance.

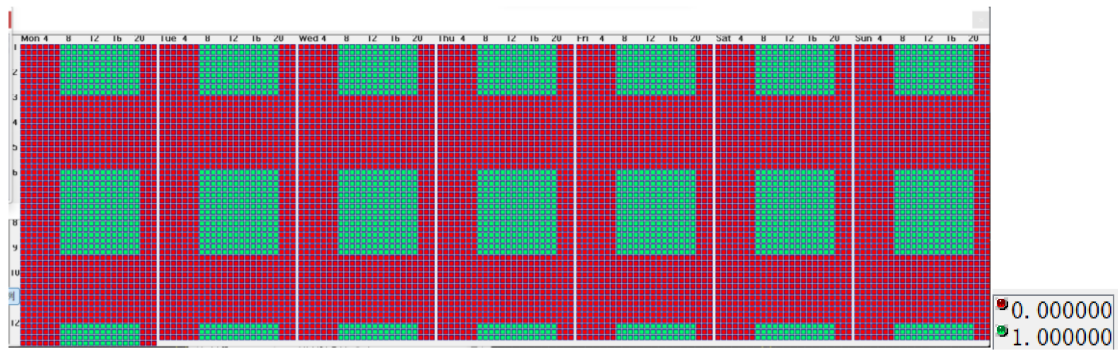


Figure 9. Air conditioning thermal disturbance in three areas.

At the same time, we set up steady-state ventilation in the model, and the number of air changes was taken as 0.4 times/h for buildings with room volumes of 2501~3000 m³, with reference to the “Unified Standard for Energy-Saving Design of Industrial Buildings” [42] (GB 51245-2017).

3. Results

3.1. Optimal Design Solution for Envelope Thermal Parameters

The building envelope was composed of three main parts, namely the exterior walls, roofs, and exterior windows. For the exterior walls and roofs, physical models were designed for twelve working conditions with the thickness of the insulation layer increasing from 0 mm to 110 mm in steps of 10 mm, and the respective heat transfer coefficients are shown in Figure 10. For the exterior windows, physical models were designed for ten working conditions, and the respective heat transfer coefficients are shown in Table 4. In this design phase, the values of the heat transfer coefficients of the envelope were fixed, and changes caused by changes in operating conditions and the outdoor environment were not considered.

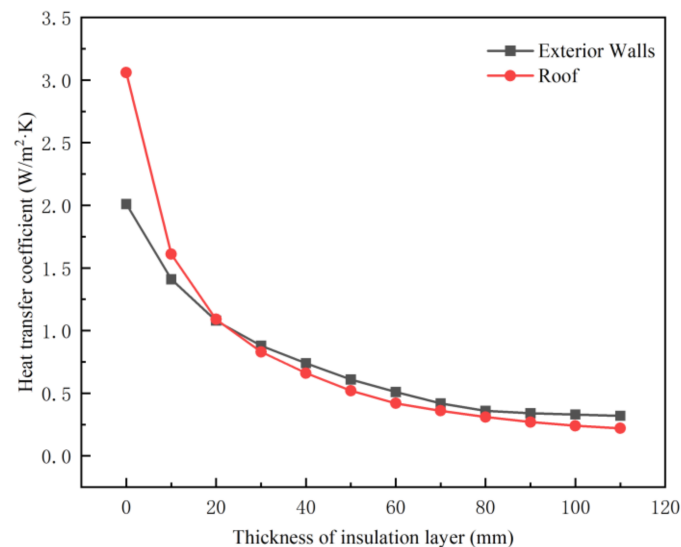


Figure 10. Heat transfer coefficients of exterior walls and roofs with different insulation layer thicknesses.

The heat transfer coefficients of one envelope part were changed individually while maintaining other parameters, and the change in building energy consumption and benefit-cost rate with the thermal properties of the envelope were obtained through computerized energy simulation, so as to seek the optimal design strategies for substations in different climate zones.

In the simulation, the heat transfer coefficients in Table 4 were entered separately in the software, and the effects of outdoor wind speed and wind direction were reflected in the weather file. Through simulation, it was found that the energy consumption of buildings in the severe cold, cold, and mild regions varied greatly, while the energy consumption of the remaining two regions were less than that in the above three regions, but the most economical and energy-saving thermal parameters of the envelope can still be obtained from them. Therefore, the most economical and energy-saving thermal parameters of substations in different climate zones were analyzed in three regions: severe cold, cold, and mild regions.

Table 4. Heat transfer coefficients of different exterior windows.

Exterior Windows	Heat Transfer Coefficient ($W/m^2 \cdot K$)
Old standard exterior window 3.50–0.80	3.50
Standard exterior window 3.2	3.20
Standard exterior window 3.00–0.80	3.00
Standard exterior window	2.80
6 (low-e) + 9 + 6	2.40
3 (low-e) + 0.1 + 3	2.20
6 (low-e) + 9 (Argon) + 6	2.00
6 + 6 air + Pet(low-e) + 6 air + 6	1.70
3 (low-e) + 0.1 + 3 + 9 + 6	1.40
6 + 6 air + Pet (low-e) + 6 air + Pet (low-e) + 6 air + 6	1.00

(1) Optimal values of envelope thermal parameters in severe cold regions

As shown in Figure 11, the total energy consumption and R_{BC} of the three types of envelopes had similar trends with the change of heat transfer coefficient. For exterior walls and roofs, when the insulation layer was thin, an appropriate increase in the thickness of the insulation layer can significantly reduce building energy consumption. However, when the thickness of exterior wall insulation reached 90~100 mm and roof insulation reached about 100 mm, the building's energy consumption was no longer significantly reduced, which meant that the energy-saving effect was limited when the thickness of the insulation layer was increased. For exterior windows, the building's energy consumption decreased linearly with the reduction of the heat transfer coefficient.

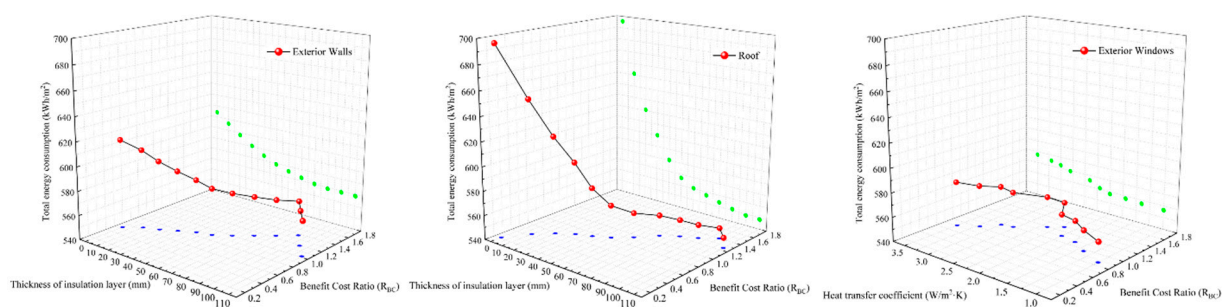


Figure 11. Variations in building energy consumption and benefit-cost rate with thermal properties of exterior walls, roofs, and exterior windows in severe cold regions.

From the economic point of view, the high energy cost brought by an insulation layer that is too thin and the surge of initial investment brought by an insulation layer that is too thick led to a significant difference in the benefit-cost rate of different insulation layers as well. From Figure 11, as the thickness of the insulation layer increased, the heat transfer coefficient decreased continuously, and the R_{BC} of all three showed a trend of rising first and then falling. When the thickness of exterior wall insulation reached 90 mm, the roof insulation thickness reached 100 mm, and the heat transfer coefficient of exterior windows

reached $2.2 \text{ W/m}^2\cdot\text{K}$, R_{BC} reached the maximum values of 1.37, 1.40, and 1.28, respectively, i.e., the envelope in such cases was the most economical.

Using the two indicators of comprehensive energy consumption and benefit-cost rate, it can be found that the most economical and energy-saving insulation layer for exterior walls in severe cold regions was 90 mm, when the heat transfer coefficient was $0.34 \text{ W/m}^2\cdot\text{K}$; the most economical and energy-saving roof insulation layer thickness was 100 mm, when the heat transfer coefficient was $0.24 \text{ W/m}^2\cdot\text{K}$. When the heat transfer coefficient of exterior windows was about $2.32 \text{ W/m}^2\cdot\text{K}$, the building had the best energy-saving effect and the lowest cost.

(2) Optimal values of envelope thermal parameters in cold regions

As shown in Figure 12, the total energy consumption and R_{BC} of the three envelopes in cold regions also had similar trends compared to those in severe cold regions. For exterior walls and roofs, when the insulation layer was thin, there was a significant reduction in building energy consumption as the thickness of insulation increased. However, when the thickness of the exterior wall insulation and roof insulation reached 70~80 mm, the trend of reducing building energy consumption slowed down significantly. When the thickness of the insulation layer was greater than this limit, there was no significant change in building energy consumption. For exterior windows, the building energy consumption decreased by different degrees with the reduction of the heat transfer coefficient. When the heat transfer coefficient of exterior windows reached $2.4 \text{ W/m}^2\cdot\text{K}$, the building energy consumption did not change much with the heat transfer coefficient.

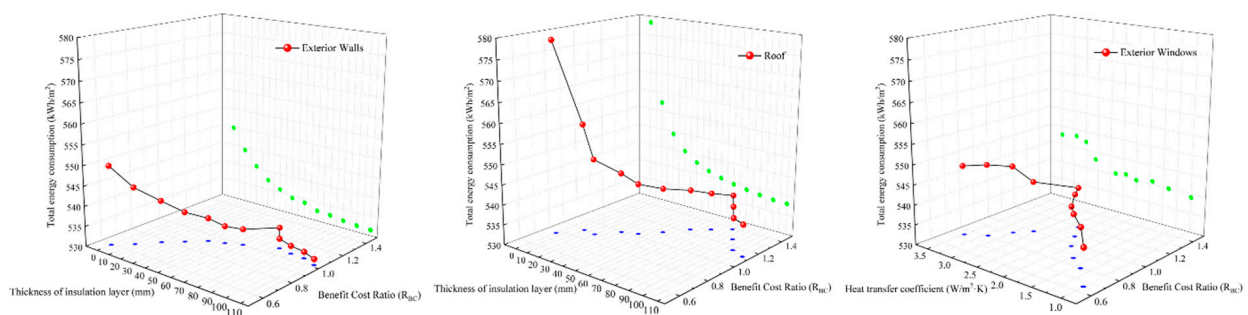


Figure 12. Variations in building energy consumption and benefit-cost rate with thermal properties of exterior walls, roofs, and exterior windows in cold regions.

From the viewpoint of economy, R_{BC} also showed different trends as the heat transfer coefficient decreased with the increase of insulation thickness. When the thickness of exterior wall insulation reached 70 mm, roof insulation reached 80 mm, and the heat transfer coefficient of exterior windows reached $2.4 \text{ W/m}^2\cdot\text{K}$, R_{BC} reached the maximum values of 1.184, 1.383, and 1.189, respectively, which meant that the envelope in such cases was the most economical.

The two indicators of comprehensive energy consumption and benefit-cost rate can be found when the thickness of the exterior wall insulation in cold areas was 70 mm and the heat transfer coefficient was $0.42 \text{ W/m}^2\cdot\text{K}$, which can achieve the purpose of economic energy saving at this time, while the optimal insulation thickness of the roof was 80 mm. In addition, when the heat transfer coefficient of exterior windows was maintained at $2.4 \text{ W/m}^2\cdot\text{K}$, it can also have an adequate energy-saving effect while ensuring economic benefits.

(3) Optimal values of envelope thermal parameters in mild regions

The simulation results for the mild regions are shown in Figure 13. From the figure, it can be seen that the change pattern in the mild regions was obviously different from that in the severe cold and cold regions, which was mainly reflected by the building energy consumption increasing instead of decreasing with the increase in insulation thickness. This was mainly due to the fact that cooling energy consumption in mild regions accounted

for a relatively large share of the total energy consumption, and the operation of equipment in substations generated a large amount of heat load, which was not conducive to heat exhaust to the outdoors when the thickness of insulation increased, leading to an increase in total energy consumption. This change law was similar in hot summer and cold winter and hot summer and warm winter regions.

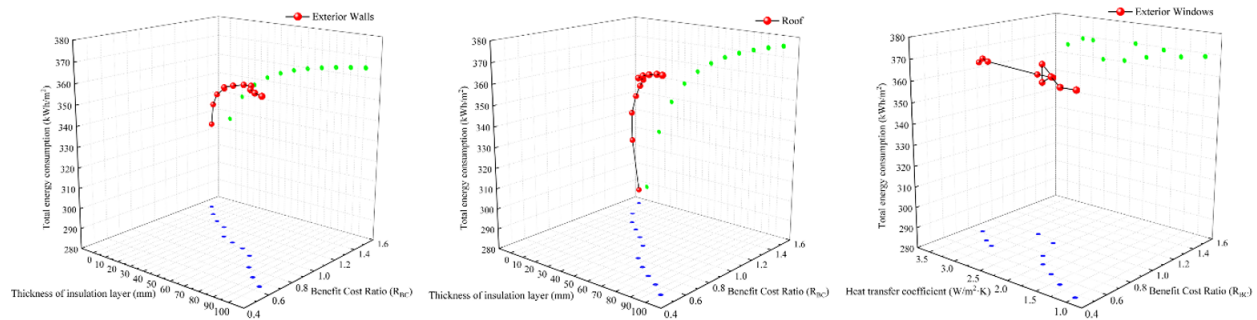


Figure 13. Variations in building energy consumption and benefit-cost rate with thermal properties of exterior walls, roofs, and exterior windows in mild regions.

As shown in Figure 13, the variation of total energy consumption and R_{BC} with the heat transfer coefficient of the envelope in the mild region was significantly different from the two regions of severe cold and cold. For exterior walls and roofs, the thicker the thickness of the insulation layer, the higher the building energy consumption would be. Therefore, in the design of exterior walls and roofs in mild regions, insulation materials with thinner and larger heat transfer coefficients should be used to promote heat exchange between indoor and outdoor areas in summer and reduce building energy consumption. Meanwhile, although the change in the heat transfer coefficient of exterior windows would cause certain fluctuations in building energy consumption, in general, the heat transfer coefficient of exterior windows had no significant effect on building energy consumption.

From the economic point of view, as the thickness of the exterior wall and roof insulation layer increased, both energy consumption cost and initial investment cost gradually increased, resulting in its R_{BC} gradually decreasing. Therefore, the most energy-saving and economical thickness threshold range of the exterior wall and roof insulation layer in mild areas was 0~10 mm, showing that the thickness of the insulation layer of the envelope should be reduced as much as possible. In addition, it can be seen from Figure 13 that when the heat transfer coefficient of exterior windows was $3.5 \text{ W/m}^2\cdot\text{K}$, the R_{BC} was the largest, and the building energy consumption at this time was also maintained at a low level. Therefore, the most economical and energy-saving heat transfer coefficient of exterior windows in mild regions should be kept at about $3.5 \text{ W/m}^2\cdot\text{K}$.

(4) Optimal threshold values for thermal parameters of envelopes in different climatic zones

Through simulation, it was found that the optimal thermal parameters of the envelope varied from one climate zone to another due to the variability of climate characteristics in each region, and the results are shown in Table 5.

In the thermal design of the envelope of low-carbon substations, the most economical and energy-saving form of envelope should be selected according to local conditions.

3.2. Optimal Design Solution for the Window-to-Wall Ratio

As an important building design parameter, the size of the window-to-wall ratio not only affects the façade effect of the building but also has a significant impact on the energy consumption of the building. China is a vast country, and the building energy consumption in different climatic zones is very different, so the window-to-wall ratio design is also different in the building design of each climatic zone. This section sought the best window-to-wall design for substations in different climatic zones by simulating the building energy consumption of typical cities in five climatic zones with different window-to-wall ratios.

Table 5. Optimal values of envelopes' thermal parameters in different climatic zones.

Climate Zones	Exterior Walls		Roofs		Exterior Windows
	Thickness of Insulation Layer (mm)	Heat Transfer Coefficient (W/m ² ·K)	Thickness of Insulation Layer (mm)	Heat Transfer Coefficient (W/m ² ·K)	Heat Transfer Coefficient (W/m ² ·K)
Severe cold	90	0.34	100	0.24	2.2
cold	70	0.42	80	0.31	2.4
Hot summer and cold winter	60	0.51	60	0.42	2.6
Hot summer and warm winter	30	0.88	50	0.52	3.0
Mild	10	1.41	10	1.61	3.5

In the field study, the window-to-wall ratios of several substations were calculated and found to fluctuate from 0.2 to 0.8 for existing substations. Therefore, in this section, a set of window-to-wall ratios was designed and the areas of windows in each direction were calculated based on the dimensions of a typical substation, as shown in Table 6. The building window-to-wall ratio was changed in the global settings of the DeST-c software and used as a variable to simulate energy consumption, while the rest of the parameters were kept the same, and the simulation results are shown in Figure 14.

Table 6. List of design values of building window-to-wall ratios.

Window to Wall Ratio	0.1	0.2	0.3	0.4	0.5
Window Area					
East window (m ²)	7.95	15.91	23.86	31.81	39.77
South Window (m ²)	11.93	23.86	35.79	47.72	59.65
West Window (m ²)	7.95	15.91	23.86	31.81	39.77
North Window (m ²)	13.92	27.84	41.76	55.68	69.60
Window to Wall Ratio	0.6	0.7	0.8	0.9	1.0
Window Area					
East window (m ²)	47.72	55.68	63.63	71.58	72.00
South Window (m ²)	71.59	83.52	95.45	107.38	136.80
West Window (m ²)	47.72	55.68	63.63	71.58	72.00
North Window (m ²)	83.52	83.52	111.36	125.28	136.80

From Figure 14, it could be seen that there was a significant effect on reducing building energy consumption by controlling the window-to-wall ratio. With the increase in the window-to-wall ratio, the building energy consumption in different climate zones showed a similar linear growth trend, but the growth rate changed slightly differently. For the severe cold regions of Harbin, the building energy consumption only increased by 5.7 kWh/m² when the window-to-wall ratio increased from 0.1 to 0.4, while the increase was much larger than 5.7 kWh/m² when the window-to-wall ratio was greater than 0.4. Therefore, the optimal window-to-wall ratio for the severe cold regions should be maintained at about 0.4. For the cold regions where Beijing is the representative city, when the window-to-wall ratio was between 0.4 and 0.5, the increase in building energy consumption was smaller, so the optimal window-to-wall ratio for this climate zone should be maintained between 0.4 and 0.5. Similarly, for hot summer and cold winter, hot summer and warm winter, and mild regions, the minimum increase in building energy consumption occurred at window-to-wall ratios of 0.3, 0.35, and 0.5, respectively. Therefore, the optimal window-to-wall ratio should be maintained at about 0.3 for hot summer and cold winter regions, between 0.3 and 0.4 for hot summer and warm winter regions, and 0.5 for mild regions.

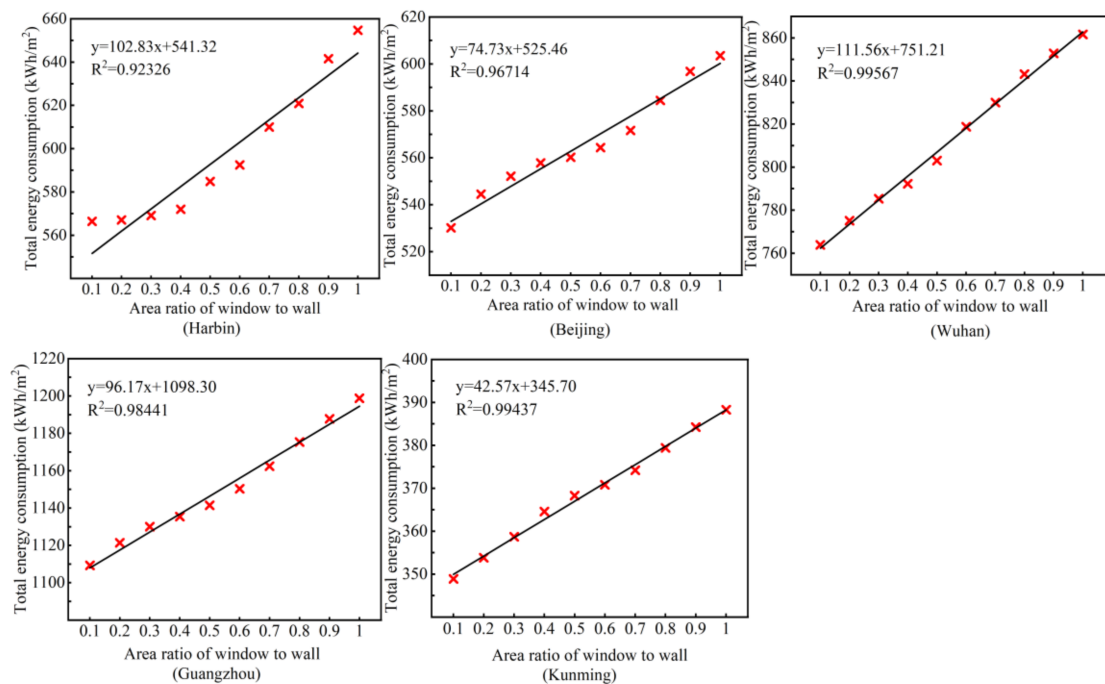


Figure 14. Variations in total building energy consumption with window-to-wall ratios in different climate zones.

3.3. Optimal Design Solutions for Shape Factors

The building shape factor is an important factor influencing the energy consumption of a building, and as the building shape factor changes, so does the energy consumption of the building. The aim of this part of the simulation was to analyze the changing pattern of building energy consumption as the building shape factor changed, and to analyze the range of shape factors that were most energy-saving for substations in different climate zones.

After field research and data queries on outdoor-type substations in severe cold regions, it was concluded that the current shape factor of the substation was about 0.35 to 0.40. Based on existing research data, this experiment was carried out for outdoor-type substations in different climatic zones by varying the height of the model's story so that the shape factor increased in steps of 0.01 between 0.33 and 0.43, while the rest of the parameters remained the same. In addition, the simulation results were fitted to a polynomial and the trends and optimum values were analyzed according to the fitting results in order to find the optimum values of the substation shape factors for different climatic zones. The simulation results are shown in Figure 15.

Based on the fitting results in Figure 15, it can be found that the fitting results for all five regions were quadratic, so the optimum shape factors for different climatic zones could be investigated based on the fitting results combined with the method of finding the optimum value of the quadratic equation. By solving the five equations above, it was found that the shape factors were taken differently for different climatic zones in order to pursue the minimum value of building energy consumption. For the severe cold regions represented by Harbin, the minimum building energy consumption was achieved when the shape factor was 0.29; For the cold regions represented by Beijing, the minimum building energy consumption was achieved when the shape factor was 0.30; For the hot summer and cold winter regions represented by Wuhan, the minimum building energy consumption was obtained when the shape factor was 0.23; For the hot summer and warm winter regions represented by Guangzhou, the minimum building energy consumption was achieved when the shape factor was 0.31, while for the mild regions represented by Kunming, the minimum building energy consumption was achieved when the shape factor was 0.33. It can be seen that the optimum shape factor varied from one climatic zone to

another. Therefore, the building design should be adapted to the geographical location of the building and different building forms should be used to maximize energy saving.

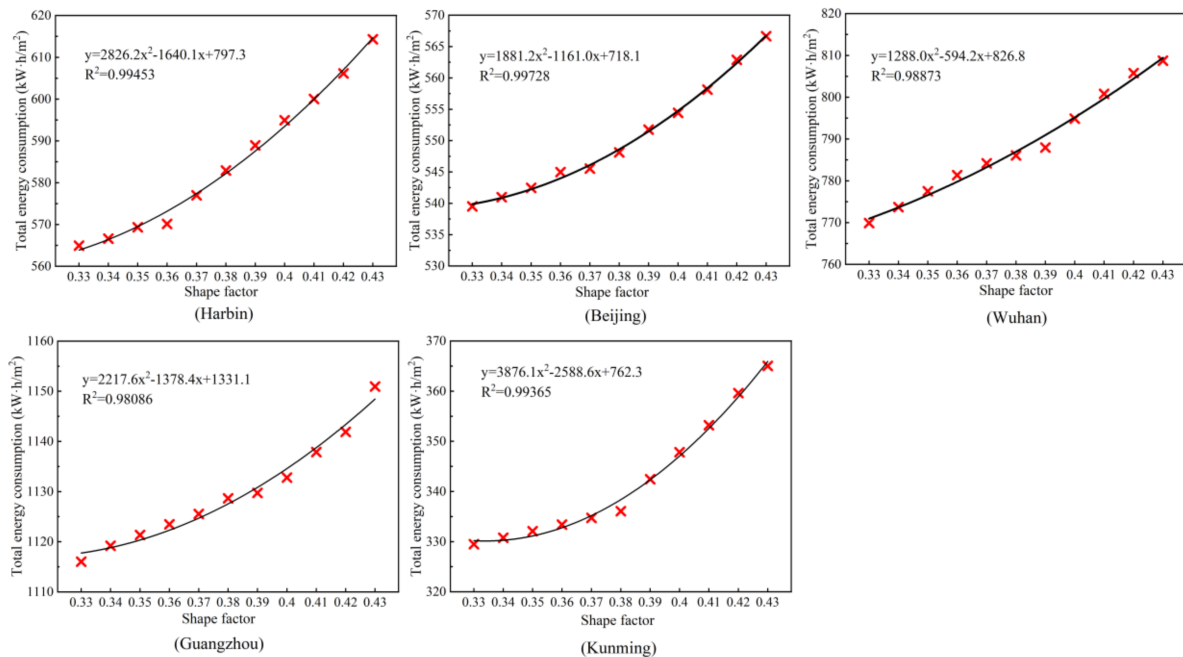


Figure 15. Variations in total building energy consumption with shape factor in different climate zones.

4. Discussion

The above study of passive design strategies for substations in different climatic zones found that the three passive strategies of changing the thermal parameters of the envelope, building window-to-wall ratio, and shape factor had significant differences in the degree of impact on building energy consumption. In order to further study the main influencing factors of building energy consumption in different climate zones, this section conducted a sensitivity analysis on the energy-saving effect of the above three passive strategies, so as to propose more accurate optimization suggestions for the relevant climate zones.

In terms of envelope design, the thickness of the roof insulation had the greatest impact on the total energy consumption of the building, the thickness of the exterior wall insulation had the second greatest impact, and the heat transfer coefficient of the exterior windows had the least impact. This was mainly due to the fact that the equipment inside the substation operated uninterruptedly throughout the day, which generated a large amount of heat. At this time, due to the building height and indoor-outdoor temperature difference, the chimney effect would be generated inside the building, which made a large amount of heat gather at the top of the building space, resulting in a large temperature difference between the inside and outside of the roof. Therefore, once the heat transfer coefficient of the roof changed slightly, it would lead to a corresponding change in the total energy consumption of the building. In other words, the energy-saving design of the roof should be focused on the thermal design of the envelope of substations in different climate zones.

In terms of building window-to-wall ratios, it can be seen from Table 5 that the sensitivity of different climate zones for different window-to-wall ratios varied. Among them, the window-to-wall ratio had the greatest impact on building energy consumption in hot summer and cold winter and severe cold regions, followed by hot summer and warm winter and cold regions, and the least impact on building energy consumption in mild regions. Therefore, the energy saving design in hot summer and cold winter regions and severe cold regions should focus on the setting of the best window-to-wall ratio, while in mild regions the building window-to-wall ratio should be reduced as much as possible to achieve the best energy-saving effect.

The effect of shape factors on building energy consumption in different regions also varied. When the shape factor fluctuated between 0.33 and 0.43, the variation of building energy consumption in severe cold regions was 49.4 kWh/m², in cold regions was 27.1 kWh/m², in hot summer and cold winter regions was 38.9 kWh/m², in hot summer and warm winter regions was 34.9 kWh/m², and in mild regions was 35.5 kWh/m². Therefore, the design process of substations in severe cold regions should focus on the setting of the optimal shape factor.

Overall, the results of this study were a guided optimization scheme applicable to both new and existing substation buildings. Of course, for existing buildings, this could only be achieved by retrofitting techniques, for which the choice is limited. Furthermore, the window-to-wall ratio in this study was a comprehensive indicator for different climate zones, and different rooms can further select different window-to-wall ratios according to their functions. At the same time, considering the actual construction and application, the insulation thickness was the same in the design, and a different insulation thickness was not considered according to the room type.

In the simulation process, this study only considered the effects of three single factors, namely the thermal physical properties of the envelope, window-to-wall ratio, and shape factor, on building energy consumption, while ignoring the coupled effects of each factor on building energy consumption. The synergistic influence of the above three factors on building energy consumption is very meaningful and worth studying. Future research will focus on different combinations of the above three factors in order to arrive at an integrated and comprehensive design strategy suitable for substations in different climate zones. In addition, combining natural and mechanical ventilation can further reduce building energy consumption, and the impact of different ventilation amounts can be considered for future studies.

5. Conclusions

In this paper, the most economical and energy-saving thermal parameters of envelopes in different climates were obtained by simulating the thermal parameters of envelopes, building window-to-wall ratios, and shape factors in typical cities in different climatic zones, and the optimal window-to-wall ratios and optimal shape factors in different climatic zones were obtained by data analysis. Through the analysis of the data, the following conclusions are summarized:

- (1) The thermal design strategy of the envelopes is different in different climate zones, and the most economical and energy-saving envelopes' thermal parameters also differ. Through simulation, it was found that in order to maximize energy savings and minimize budget investment in substation buildings, each region should choose the most suitable thermal parameters of envelopes according to local conditions. Among the envelopes, the thickness of the roof insulation had the greatest influence on the energy consumption of substation buildings, the thickness of the exterior wall insulation was the second, and the heat transfer coefficient of exterior windows had the least influence on the energy consumption of buildings.
- (2) Low-carbon substations selected the optimal window-to-wall ratio to effectively reduce the comprehensive energy consumption of the building, and the optimal window-to-wall ratio for substations in different climate zones was different. The optimal window to wall ratio should be maintained at around 0.4 in severe cold regions, 0.4~0.5 in cold regions, 0.3 in hot summer and cold winter regions, 0.3~0.4 in hot summer and warm winter regions, and 0.5 in mild regions. In particular, in the hot summer and cold winter regions and severe cold regions, special attention should be paid to the selection of the optimal window-to-wall ratio.
- (3) The geometry of the building should be designed to maximize the energy-saving effect of the building. The optimal shape factor for severe cold regions was 0.29, 0.30 in cold regions, 0.23 in hot summer and cold winter regions, 0.31 in hot summer and

warm winter regions, and 0.33 in mild regions. Among them, the shape factor had the greatest influence on building energy consumption in cold regions.

- (4) Energy efficiency optimization strategies for substations vary greatly from one climate zone to another. In terms of the thermal design of the enclosure, colder regions should use thicker insulation materials to reduce the heat exchange between the interior and exterior. On the contrary, in hot and humid regions, the thickness of the insulation material should be reduced as much as possible to maximize the energy saving of the building. In terms of the building's physical design, the window area in cold areas should not be too large to prevent heat outflow, while in hot and humid areas, a larger window area should be controlled. In addition, the design of geometric dimensions should also be adapted to local conditions, and the building form factor should be reasonably controlled.

Author Contributions: Conceptualization, S.Z. and G.C.; Methodology, H.S.; Software, S.Z.; Validation, J.S., Z.X. and Y.L.; Formal analysis, J.S.; Investigation, L.Y.; Resources, S.Z.; Data curation, J.S.; Writing—original draft, S.Z.; Writing—review and editing, G.C.; Visualization, Y.L.; Supervision, H.S. and L.Y.; Project administration, S.Z.; Funding acquisition, Z.X. All authors have read and agreed to the published version of the manuscript.

Funding: This research was funded by the Collective Enterprise Science and Technology Project (CY840800JS20230018) of State Grid Huzhou Electric Power supply company State Grid Zhejiang Electric Power supply Company, LTD, Huzhou 313000, China.

Data Availability Statement: Data are available on request due to restrictions. The data presented in this paper are available on request from the corresponding author.

Acknowledgments: This article was supported by State Grid Huzhou Electric Power supply company State Grid Zhejiang Electric Power supply Company, LTD, Huzhou 313000, China.

Conflicts of Interest: The authors declare no conflict of interest.

Abbreviations

ρ_{in}	Indoor air density	kg/m ³
V_{in}	Indoor air volume	m ³
c_{in}	Specific heat of air	kJ/kg·K
T_{in}	Indoor air temperature	K
t	Time analyzed	s
$\sum Q_{env}$	The total heat transfer from the envelope to the room	kW
$\sum Q_{conv}$	The total convection heat dissipation from the indoor heat source	kW
$\sum Q_{AC}$	The total heat supplied to the room by the air conditioning system	kW
$\alpha_{env,i}$	Convective heat transfer coefficient of the inner surface of the outer envelope	W/m ² ·K
$T_{env,i}$	Temperature of the inner surface of the outer envelope	K
A_{env}	Surface area of the envelope	m ²
q_{out}	The sum of the total heat gain of the outer surface of the outer envelope	W/m ²
$q_{cond,o}$	The sum of all heat gains from thermal conduction of the outer surface of the outer envelope	W/m ²
$q_{cond,i}$	The sum of all heat gain from thermal conduction of the inner surface of the outer envelope	W/m ²
$q_{solar,i}$	The sum of all the heat from sunlight entering the room with windows on the inner surface of the outer envelope	W/m ²
$q_{rad,i}$	The heat obtained from the inner surface by radiation from an internal heat source	W/m ²
$q_{conv,i}$	The convective heat exchange between the inner surface and the room air	W/m ²
T_{env}	The temperature of the outer envelope at time t and distance x_{env}	K

a_{env}	Heat diffusion coefficient inside the outer envelope	m^2/s
x_{env}	Location of the outer envelope analyzed at time t	m
σ_{env}	Thickness of the outer envelope	m
$\lambda_{env,o}$	Thermal conductivity of the outer surface of the outer envelope	$W/m \cdot K$
$\lambda_{env,i}$	Thermal conductivity of the inner surface of the outer envelope	$W/m \cdot K$
γ_{env}	The proportion of solar radiation received by the inner surface of the outer envelope to the total incident radiation	
$\alpha_{env,rad,i}$	Radiant heat transfer coefficient of the inner surface of the outer envelope	$W/m^2 \cdot K$
$T_{ave,i}$	Average temperature of inner surfaces other than the analyzed surface	K
κ_{env}	The ratio of the radiant heat transfer from indoor heat sources received by the inner surface of the outer envelope to the total radiant heat dissipation from indoor heat sources	
T_{out}	Outside air temperature	K
$T_{env,o}$	Outer surface temperature of the outer envelope	K
$T_{env,i}$	Inner surface temperature of the outer envelope	K
α_{env}	Convective heat transfer coefficient of the outer surface of the outer envelope	$W/m^2 \cdot K$
$Q_{solar,i}$	Total indoor solar heat radiation	kW
Q_{rad}	Total indoor heat source radiation heat dissipation	kW
N	Calculation period	
t	Year	
B	Economic benefits	
B_t	Economic benefits in year t	
C_0	Initial costs	
C_N	Dismantling costs	
C_t	Operation and maintenance costs	
d	Social discount rate	
e	Average annual growth rate of energy prices	
R_{BC}	Benefits to Cost Ratio	
$DeST-C$	Designer's Simulation Toolkit-Commercial	
LCB	Life Cycle Benefits	
LCC	Life Cycle Cost	

References

1. IEA. *Key World Energy Statistics 2016*; IEA: Paris, France, 2016. [\[CrossRef\]](#)
2. Holmatov, B.; Hoekstra, A.Y.; Krol, M.S. Land, water and carbon footprints of circular bioenergy production systems. *Renew. Sustain. Energy Rev.* **2019**, *111*, 224–235. [\[CrossRef\]](#)
3. Elshkaki, A. The implications of material and energy efficiencies for the climate change mitigation potential of global energy transition scenarios. *Energy* **2023**, *267*, 126596. [\[CrossRef\]](#)
4. Guo, J.H. Introduction to the application of energy saving technology in substations. *Shanxi Archit.* **2010**, *36*, 248–249. [\[CrossRef\]](#)
5. Li, S.Q. Construction and Empirical Study of Energy Saving Assessment System for Substation Construction Projects. Master's Thesis, North China Electric Power University, Baoding, China, 2012.
6. Feng, Z.; Zhang, G.; Wu, J.; Han, W.; Fang, S.; Yan, X.; Huang, S. Research on corona characteristics and type selection of fittings in extra high voltage alternating current substation. *Energy Rep.* **2022**, *8*, 176–186. [\[CrossRef\]](#)
7. Zhang, X.; Liu, L.Q.; Wu, M.L.; Wang, W.; Chen, G.; Yan, W.; Cao, M.; Liang, H.S.; Zhang, C.S.; Chen, B.; et al. Research and application of energy efficiency assessment and energy saving retrofit technology for substations. *Power Ind.* **2019**, *470*, 40.
8. China Electricity Council Technical and Economic Consulting Center for Electricity Construction. *Substation Building Engineering*; China Electric Power Press: Beijing, China, 2008.
9. Du, C. Research on Substation Building Design. Master's Thesis, Shenyang Jianzhu University, Shenyang, China, 2020. [\[CrossRef\]](#)
10. Wang, Y.F. Research on Energy Saving Design of Substation Buildings in Severe Cold Regions Based on Computer Simulation. Master's Thesis, Harbin Institute of Technology, Harbin, China, 2013.
11. Chen, Z.; Sun, D.W. Analysis of factors affecting energy consumption of buildings in China. *Ind. Technol. Forum* **2008**, *6*, 150–151.
12. Nie, J.C.; Zhang, Z.; Zhang, X.Y.; SaRen, G.W.; Luo, D.M. Energy saving design of substation buildings in Inner Mongolia. *Imm. Mong. Electr. Power Technol.* **2018**, *36*, 43–50.
13. Ybyraiymkul, D.; Chen, Q.; Burhan, M.; Akhtar, F.H.; AlRowais, R.; Shahzad, M.W.; Ja, M.K.; Ng, K.C. Innovative solid desiccant dehumidification using distributed microwaves. *Sci. Rep.* **2023**, *13*, 7386. [\[CrossRef\]](#) [\[PubMed\]](#)
14. Krarti, M.; Ybyraiymkul, D.; Ja, M.K.; Burhan, M.; Chen, Q.; Shahzad, M.; Ng, K. Energy performance of hybrid evaporative-vapor compression air conditioning systems for Saudi residential building stocks. *J. Build. Eng.* **2023**, *69*, 106344. [\[CrossRef\]](#)
15. Wolfgang, F.; Guo, L.; Sheng, S.C.; Jiang, H.J. Passive house in China: Health, Comfort, affordability and sustainability. *Eco-City Green Build* **2016**, *3*, 31–37.

16. Liu, H.Z.; Ding, H.T.; Li, T.Y.; Guo, Y.Y.; Zhao, G.P. Research on building energy consumption status of Civil buildings and development trend in China. *Build. Technol.* **2018**, *8*, 10–11. [[CrossRef](#)]
17. Lin, Y.L.; Zhao, L.Q.; Yang, W.; Hao, X.L.; Li, C.Q. A review on research and development of passive building in China. *J. Build. Eng.* **2021**, *42*, 102509. [[CrossRef](#)]
18. Brito-Coimbra, S.; Aelenei, D.; Gloria Gomes, M.; Moret Rodrigues, A. Building Façade Retrofit with Solar Passive Technologies: A Literature Review. *Energies* **2021**, *14*, 1774. [[CrossRef](#)]
19. Kini, P.G.; Garg, N.K.; Kamath, K. An assessment of the impact of passive design variations of the building envelope using thermal discomfort index and energy savings in warm and humid climate. *Energy Rep.* **2022**, *8*, 616–624. [[CrossRef](#)]
20. Mushtaha, E.; Salameh, T.; Kharrufa, S.; Mori, T.; Aldawoud, A.; Hamad, R.; Nemer, T. The impact of passive design strategies on cooling loads of buildings in temperate climate. *Case Stud. Therm. Eng.* **2021**, *28*, 101588. [[CrossRef](#)]
21. Jung, Y.J.; Heo, Y.; Lee, H. Multi-objective optimization of the multi-story residential building with passive design strategy in South Korea. *Build. Environ.* **2021**, *203*, 108061. [[CrossRef](#)]
22. Pajek, L.; Kosir, M. Strategy for achieving long-term energy efficiency of European single-family buildings through passive climate adaptation. *Appl. Energy* **2021**, *297*, 117116. [[CrossRef](#)]
23. Li, E.; Liu, J.P.; Yang, L. Research on the passive design optimization of direct solar gain house for residential buildings in Lhasa. *Ind. Constr.* **2012**, *42*, 27–32. [[CrossRef](#)]
24. Yin, M.Z. Adaptability Analysis of Passive House in the Northern Part of China. Master's Thesis, Shandong Jianzhu University, Jinan, China, 2016.
25. Zhang, S.L. Research on Methods of Passive House Design for Congregate Housing in Cold Region. Master's Thesis, Hebei University of Technology, Tianjin, China, 2015.
26. Kang, J.; Yin, X. Energy saving design of 500 KV substation building. *Jilin Electr. Power* **2013**, *41*, 27–28. [[CrossRef](#)]
27. Zhang, G.L.; Zhao, S.Y.; Wang, N.; Zhao, B.J. Research on the application of passive building technology in the extra-high voltage substation buildings. *Constr. Technol.* **2018**, *37*, 18–26. [[CrossRef](#)]
28. Yang, X.P. Research on Ventilation and Air Conditioning System of Underground Substation and Energy Saving Optimization. Master's Thesis, Donghua University, Shanghai, China, 2011.
29. Wang, W.B.; Hua, B. Research on energy saving of automatic control of air conditioning system in substation. *East China Electr. Power* **2009**, *37*, 777–780.
30. Xiong, T.J.; Li, G.P.; Liu, Y.; Li, S.J. Research on ways to achieve near-zero energy substation buildings. *Build. Energy Effic.* **2021**, *12*, 39–44.
31. Zhang, C. Building optimization innovation and energy saving and environmental protection. *Build. Energy Sav.* **2014**, *51*, 239–240.
32. Liu, Y.F.; Zhang, Y.F.; Cai, Z.H.; Zhang, J.; Liu, Q.N. Influence of thermal parameters of outer envelope on energy consumption of substation buildings. *Build. Energy Sav.* **2020**, *2*, 29–33.
33. Zhou, S.R. Energy saving design of substation buildings in mild regions. *Sci. Technol. Innov. Her.* **2015**, *28*, 93–94. [[CrossRef](#)]
34. Lin, Y.L.; Zhang, F. Energy saving design of substation buildings in hot summer and cold winter regions. *Shanxi Archit.* **2009**, *35*, 238–240.
35. Zhang, S.J.; Zhang, J.B.; Du, H.B. Energy saving testing of substation buildings in severe cold regions. *Heilongjiang Sci.* **2014**, *5*, 70–71.
36. Han, X.L.; Chen, B.; Zhu, J.Y. Economic Analysis and Case Study of Building Thermal Design Optimization. *Build. Sci.* **2014**, *30*, 65–71. [[CrossRef](#)]
37. Ministry of Construction, National Development and Reform Commission. *Methods and Parameters for Economic Evaluation of Construction Projects*, 3rd ed.; China Planning Press: Beijing, China, 2006.
38. Xie, X.N.; Song, F.T.; Yan, D.; Jiang, Y. Building environment design simulation software DeST(2): Dynamic thermal process of buildings. *Heat. Vent. Air Cond.* **2004**, *34*, 35–47.
39. Zhu, D.D.; Yan, D.; Wang, C. Comparison of Building Energy Simulation Programs: DeST, EnergyPlus and DOE-2. *Build. Sci.* **2012**, *28*, 213–222. [[CrossRef](#)]
40. GB 50176-2016; Thermal Design Code for Civil Buildings. China Construction Industry Press: Beijing, China, 2016.
41. DL/T 5218-2012; Technical Regulations for the Design of 220 kV~750 kV Substations. China Plan Press: Beijing, China, 2012.
42. GB 51245-2017; Unified Standard for Energy-Saving Design of Industrial Buildings. China Plan Press: Beijing, China, 2017.

Disclaimer/Publisher's Note: The statements, opinions and data contained in all publications are solely those of the individual author(s) and contributor(s) and not of MDPI and/or the editor(s). MDPI and/or the editor(s) disclaim responsibility for any injury to people or property resulting from any ideas, methods, instructions or products referred to in the content.